Physical Modelling in Geotechnics

Centrifuge modelling for dynamic behaviour of shallow foundation on liquefied soil: Effect of amplitude and duration of earthquake motion

D.H. Choi & T.H. Kwon
Department of Civil & Environmental Engineering, KAIST, Daejeon, Korea

K.W. Ko
Department of Civil & Environmental Engineering, U.C. Berkeley, U.S.

ABSTRACT: Liquefaction can occur in saturated loose sands and cause significant ground settlement and rotation of superstructures. Structures on liquefied soil are exposed to the volumetric-induced settlement, deviatoric-induced settlement, and soil ejecta (sand boil). However, ground deformation and seismic behaviour of shallow foundations associated with the seismic ground motion remains poorly understood. Therefore, this study aims to evaluate the effect of earthquake characteristics on the dynamic behaviours of a shallow foundation and liquefaction-associated ground settlement via dynamic centrifuge modelling. The results show clear evidence of liquefaction and associated ground settlement in the free field where no foundation is placed. By contrast, the ground under the foundation is not liquefied, but more significant deformation occurs due to the overlying structural weight. It is found that the duration, rather than the peak amplitude of the earthquake, has a profound effect on the settlement of an overlying structure. On the other hand, the peak amplitude of earthquakes is closely related to the rotation of the superstructure. The present study provides clear physical modelling results on the role of earthquake characteristics in the dynamic behaviour of the soil-foundation-structure-interaction (SFSI) on the liquefied ground.

Keywords: Centrifuge test, Earthquake motion, Liquefaction, Shallow foundation, Deformation.

1. INTRODUCTION

The encounter between liquefaction and structure can cause disastrous consequences (Seed and Idriss, 1967; Boulanger et al., 1997; Holzer et al., 1999). When liquefaction-induced damage is mostly related to the settlement or rotation of structures. Three major mechanisms are classified to understand the soil-foundation-structure-interaction (SFSI) mechanisms of this complex consequence: volumetric deformation (ε_p), deviatoric deformation (ε_q), and soil ejecta (ε_{EJT}) (Dashti et al. 2010; Bray and Dashti, 2014; Luque and Bray 2017;). It is still unclear the role of input earthquake characteristics in the ground deformation of saturated liquefiable sands. Furthermore, the rotational behaviour of the structure due to the seismic motion remains poorly examined.

Therefore, this study investigated the dynamic behaviours of soil and structures under different earthquake motions. Furthermore, not only settlement of ground and structure but also rotation of structure was analysed.

2. CENTRIFUGE MODELLING

2.1 Centrifuge test description

The centrifuge facility of KAIST used in this study is a 240 g-tons asymmetric beam centrifuge with a 5 m radius, which can accelerate the 2400 kg models at 100 g-level centrifugal acceleration. Besides, the shaking table is designed to operate under 100g centrifugal acceleration and the maximum shaking acceleration level of 20g at the model scale (Kim et al., 2013).

Total two centrifuge model tests were carried out, only varying the input earthquake motion. The first test used a long duration and weak amplitude motion (LDWM), and the second test was subjected to a short duration and strong amplitude motion (SDSM). We chose the Korean acceleration standard design spectrum for the S1 ground (rocky ground) (KDS 17 10 00:2018) to keep the spectral response and the dominant frequency consistent between the tests (Fig.1). As a result, LDWM had a duration of 18 s and a PGA of 0.154 g, while SDSM had a 5 s and a 0.22 g. Additionally, the Arias intensity of each motion was 0.23 m/s and 0.16 m/s, respectively.

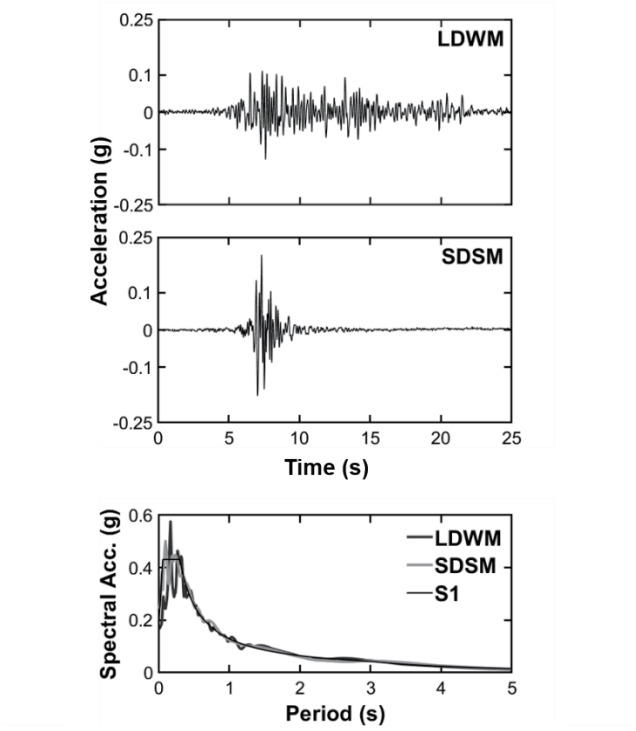

Fig. 1. Input earthquake motions.

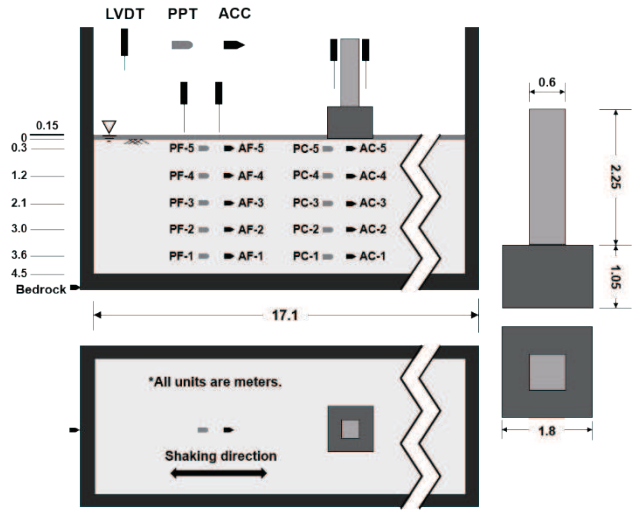

Fig. 2. Test model (all units are meters as the prototype scale at 30g). In the LDWM test, the sensors were installed only at the depths of 0.3 m, 2.1 m, and 3.6 m, respectively. The figure is not drawn to scale.

Because the seismic excitation causes ground disturbance and alters soil properties in the model, each model was subjected to only one input motion in each experimental case. We used the g-level of 30g, and accordingly, the rigid model box had the dimension of 17.1 m × 7.05 m × 14.64 m (L × W × H) as the prototype model. The weight of a single-degree-of-freedom shallow foundation model was 41.07 kN as a prototype, and the dimension is detailed in Fig. 2. The pore water pressure transducer (P) and the accelerometer (A) were arranged in two rows, and their positions were divided into 'free field (F)' and 'centre (C)', respectively. Furthermore, the LVDTs were installed on the ground and foundation surface to measure the settlement as well as rotation.

2.2 Ground model

The silica sand was pluviated using automatic pluviation equipment to match the initial relative density 45% for ground modelling (Table.1). We prepared the viscous fluid by using the 'Hot/Cold method' and HPMC powder in accordance with the scaling law of diffusion and controlled the fluid viscosity more accurately considering the temperature and g-level of the centrifuge chamber (Dewoolkar et al., 1999; Adamidis and Madabhushi, 2015).

Thereafter, the circulation process was progressed to produce a vacuum state in the vacuum chamber. We set the vacuum pressure inside the vacuum chamber to -95 kPa, then injected carbon dioxide gas until the pressure rises to +30 kPa to eliminate any remaining air. Before readjusting the pressure to -95 kPa, we waited until the airflow within the vacuum chamber was stabilized. This procedure was repeated at least twice to ensure the removal of air and an effective vacuum state, which is critical to constructing a liquefaction soil model.

After the circulation, the saturation process was carried out in a vacuum state, and the prepared viscous fluid dropped to the surface of the ground at a rate of 2 mL/min. In the end, we validated the saturation state using the Okamura method and achieved a saturation over 99.9% (Okamura and Inoue, 2012). Any tiny air bubble in the soil decreases the degree of saturation of the soil model, and even a little decrease in saturation, of the order of a few per cent, enhances the liquefaction resistance of clean sands (Yoshimi et al., 1989).

Table 1. Soil properties

Property	Value
Specific gravity, G_s	2.65
Initial relative density, D_r (%)	45
Median diameter, D_{50} (mm)	0.235
Coefficient of curvature, C_c	1.03
Uniformity coefficient, C_u	1.76

3. CENTRIFUGE TEST RESULTS

All results are expressed with respect to the prototype scale. We determine the settlement from the averaged displacement value from two LVDTs installed on the ground surface or the surface of the foundation structure. The difference between the two vertical displacements determines the structure rotation.

3.1 Evidence of liquefaction

Liquefaction mainly occurs due to shear strength loss, caused by upward fluid flow related to excess pore water pressure (Δu_{ex}) generation. The most representative engineering parameter of liquefaction triggering is the ratio of excess pore water pressure (R_u), defined as

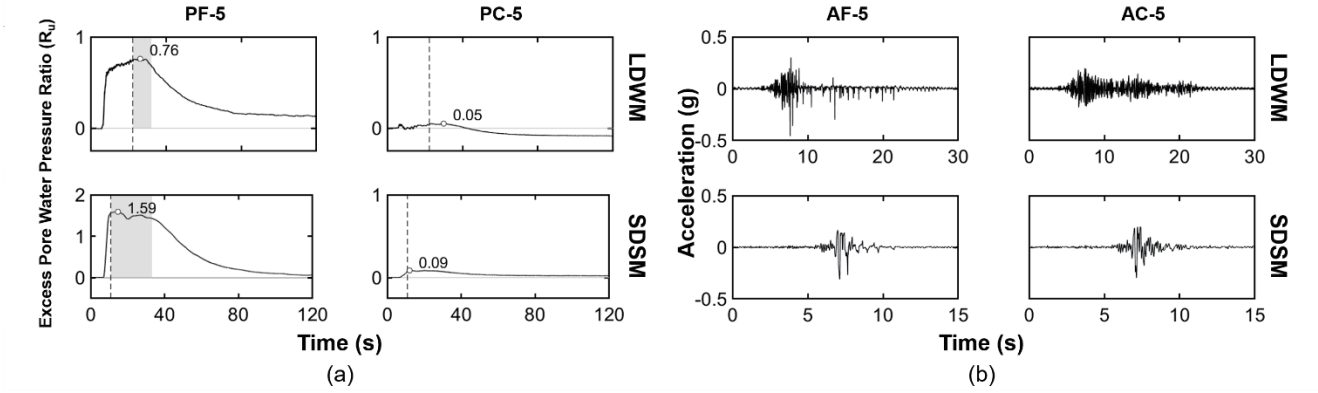

Fig. 3. Comparison of liquefaction evidence: (a) Time – R_u history, and (b) Time – Acceleration history. The vertical dashed line in the subplot (a) indicates the end of shaking.

the ratio of excess pore water pressure to initial vertical effective stress (σ'_{v0}):

$$R_u = \frac{\Delta u_{ex}}{\sigma'_{v0}} \ . \quad (1)$$

First, let us examine the R_u value if the R_u value rises close to 1 to infer the occurrence of liquefaction. Fig. 3a shows the R_u histories of both tests. The maximum R_u values at PF-5 in the free field were 0.76 and 1.59, respectively, which indicates that the liquefaction occurred in the free field. Note that the R_u value greater than 1 is possibly attributable to various experimental errors, including the uncertainty in direction and position change of sensors during spin-up or seismic shaking. By contrast, the maximum R_u values at PC-5 (under the foundation structure) both Cases LDWM and SDSM were 0.05 and 0.09, respectively. It demonstrates that the increased effective stress by the shallow foundation hindered the liquefaction.

Second, the liquefaction occurrence can be also inferred from the presence of a residual state of excess pore water pressure. This is the period during which the R_u value remains at over 90% of the maximum value after the end of shaking, i.e., the grey-coloured part at PF-5 in Fig. 3a. This is because the excess pore water pressure continues to dissipate to the surface even after the main shaking is over. This state persisted for 8.3 s in Case LDWM and for 22.2 s in Case SDSM, respectively, as shown in Fig. 3a. The residual state of excess pore water pressure also supports that the liquefaction occurred in the free field for both Cases LDWM and SDSM.

Third, the liquefaction can be inferred from the dilation spike and flat response in the acceleration history. These signatures are the results of the momentary shear strength recovery during the liquefaction due to the state of phase transformation (Ishihara et al., 1975) or quasi-steady-state (QSS) (Alarcon-Guzman et al., 1988). Both the cases LDWM and SDSM showed dilation spikes at AF-5 while no distinct spike appeared at AC-5 (Fig. 3b), which are consistent with the previous observations from the R_u value and the residual excess pore water pressure.

3.2 Deformation and rotation

The settlements at the free field were -5.0 mm in Case LDWM and -4.7 mm in Case SDSM, respectively, as shown in Fig. 4a. Although the amplitude and duration of the two input motions were significantly different, the resulting settlements in the free field were almost the same. This is possibly attributable to the fact that the energy level of the input motion, such as Arias intensity, was in the comparable level to each other.

By contrast, the settlement at the shallow foundation was as large as -21.4 mm for Case LDWM and -15.5 mm for Case SDSM, respectively. Apparently, the greater settlement occurred in Case LDWM. This is presumably because the longer the duration, the more cycles were delivered to the ground, resulting in the more severe settlement, despite the smaller PGA. The settlement began with the initiation of shaking and lasted until the end of the shaking. These results may be related to the partial bearing failure in deviatoric deformation.

Contrary to the settlement, the structure rotation appears to gain more relevance to the amplitude rather than the duration of earthquake motion. The SDSM motion caused the permanent rotation of -0.07° while only minimal rotation took place with the LDWM motion (Fig. 4b). It is interesting to point out that in both cases, the rotation began to accumulate after the peak acceleration until the end of the shaking (EOS), though the rotational direction in Case LDWM changed during shaking (Figs. 4c and 4d). By contrast, from the initial excitation to the Peak, the rotation hardly took place, but the settlement began accumulating and continued after EOS. This observation implies that the rotational behaviour of shallow foundations somewhat differs from the settlement behaviour of the ground. Note that the observed rotation is in a fairly small range, less than 0.1 degrees at the prototype scale, and caution is required to extend our result to greater rotations.

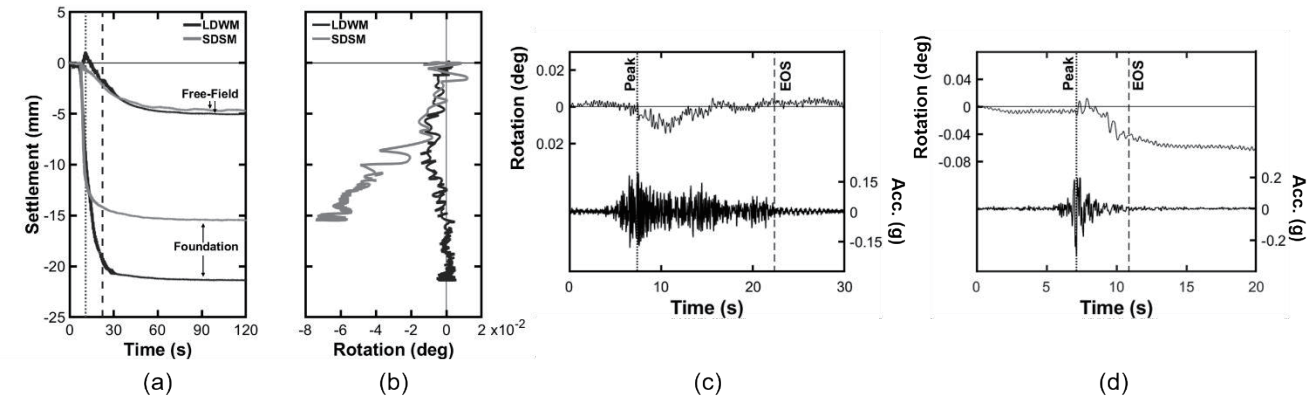

Fig. 4. Deformations: (a) Time – Settlement, (b) Rotation – Settlement, (c) & (d) Rotation and Acceleration history of LDWM and SDSM at AC-5, respectively. 'Peak' means PGA time and 'EOS' means end-of-shaking. A negative value means settlements and counter-clockwise rotation.

4. CONCLUSION

This study investigated the effect of amplitude and duration of input motion on the dynamic behaviours of ground and shallow foundation. Two same soil models were constructed by the silica sand which had 45 % of relative density. The input earthquake motions were spectrally matched to eliminate the effect of dominant frequency difference. One input motion had a long duration with a small PGA (LDWM), and the other had a short duration but with a large PGA (SDSM). The liquefaction occurred at the shallow depth in the free field, but not under the shallow foundation due to overburden stress. The settlement at both tests showed no difference in the free field. However, at the shallow foundation, Case LDWM was more settled, because of its higher duration which is related to the cycle of earthquake motion. Furthermore, the structure rotation had occurred more in Case SDSM, which was affected by the peak amplitude rather than the duration. We hope that this can serve as a cornerstone for future researches on liquefaction damage mitigation.

ACKNOWLEDGEMENTS

This research was supported by UNDERGROUND CITY OF THE FUTURE program funded by the Ministry of Science and ICT.

REFERENCES

Adamidis, O., & Madabhushi, G. S. P. (2015). Use of viscous pore fluids in dynamic centrifuge modelling. International Journal of Physical Modelling in Geotechnics, 15(3), 141-149.

Alarcon-Guzman, A., Leonards, G. A., & Chameau, J. L. (1988). Undrained monotonic and cyclic strength of sands. Journal of Geotechnical Engineering, 114(10), 1089-1109.

Boulanger, R. W., Mejia, L. H., & Idriss, I. M. (1997). Liquefaction at moss landing during Loma Prieta earthquake. Journal of Geotechnical and Geoenvironmental Engineering, 123(5), 453-467.

Bray, J. D., & Dashti, S. (2014). Liquefaction-induced building movements. Bulletin of Earthquake Engineering, 12(3), 1129-1156.

Dashti, S., Bray, J. D., Pestana, J. M., Riemer, M., & Wilson, D. (2010). Mechanisms of seismically induced settlement of buildings with shallow foundations on liquefiable soil. Journal of geotechnical and geoenvironmental engineering, 136(1), 151-164.

Dewoolkar, M. M., Ko, H. Y., Stadler, A. T., & Astaneh, S. M. F. (1999). A substitute pore fluid for seismic centrifuge modeling. Geotechnical Testing Journal, 22(3), 196-210.

Elgamal, A. W., Dobry, R., Parra, E., & Yang, Z. (1998, March). Soil dilation and shear deformations during liquefaction. In Proceedings 4th Intl. Conf. on Case Histories in Geotechnical Engineering (pp. 1238-59).

Holzer, T. L., Bennett, M. J., Ponti, D. J., & Tinsley III, J. C. (1999). Liquefaction and soil failure during 1994 Northridge earthquake. Journal of Geotechnical and Geoenvironmental Engineering, 125(6), 438-452.

Ishihara, K., Tatsuoka, F., & Yasuda, S. (1975). Undrained deformation and liquefaction of sand under cyclic stresses. Soils and foundations, 15(1), 29-44.

Kim, D. S., Kim, N. R., Choo, Y. W., & Cho, G. C. (2013). A newly developed state-of-the-art geotechnical centrifuge in Korea. KSCE journal of Civil Engineering, 17(1), 77-84.

Luque, R., & Bray, J. D. (2017). Dynamic analyses of two buildings founded on liquefiable soils during the Canterbury earthquake sequence. Journal of Geotechnical and Geoenvironmental Engineering, 143(9), 04017067.

Ministry of Land, Infrastructure and Transport (MLIT) (2018). General seismic design (KDS 17 10 00), Ministry of Land, Infrastructure and Transport, Korea (in Korean).

Okamura, M., & Inoue, T. (2012). Preparation of fully saturated models for liquefaction study. International Journal of Physical Modelling in Geotechnics, 12(1), 39-46.

Seed, H. B., & Idriss, I. M. (1967). Analysis of soil liquefaction: Niigata earthquake. Journal of the Soil Mechanics and Foundations Division, 93(3), 83-108.

Yoshimi, Y., Tanaka, K., & Tokimatsu, K. (1989). Liquefaction resistance of a partially saturated sand. Soils and foundations, 29(3), 157-162.

Zeghal, M., Goswami, N., Kutter, B. L., Manzari, M. T., Abdoun, T., Arduino, P., ... & Ziotopoulou, K. (2018). Stress-strain response of the LEAP-2015 centrifuge tests and numerical predictions. Soil Dynamics and Earthquake Engineering, 113, 804-818.